PERGAMON

Carbon 38 (2000) 1863–1871

CARBON

Intermolecular interactions of aromatic hydrocarbons in carbonaceous materials
A molecular and quantum mechanics

Anna Marzec*

Institute of Coal Chemistry — Polish Academy of Sciences, Sowinskiego 5, 44-121 Gliwice, Poland

Received 23 August 1999; accepted 8 January 2000

Abstract

Aromatic hydrocarbons (PAHs and oligomers) that are models of carbonaceous materials components were studied using MM+All Atom Force Field and the semi-empirical methods (MINDO3 and ZINDO1) of quantum chemistry. The following intermolecular interactions were studied through potential energy function: (i) Among PAH molecules; (ii) among oligomeric molecules; and (iii) among oligomer and PAH molecules. (i) The potential energy minimized stacks of PAHs showed interlayer distances which correspond to the experimentally measured distances in carbonaceous materials. (ii) Interactions among oligomers, in general, resulted in aggregates that showed random space orientation of aromatic units. Only few aromatic units of separate oligomers were parallel to each other. (iii) Interactions among the oligomer and PAH molecules resulted in parallel orientation of PAH molecules relative to aromatic units of the oligomer. Common orbitals were found in stacks of parallel oriented aromatic planes, no matter whether the planes belonged to individual molecules forming PAH crystallites, oligomeric aggregates, or PAH/oligomer aggregates. Conclusions refer to the chemical structure of the optical isotropy phase occurring in carbonaceous materials, electrical conductivity of the materials, and X-ray measurements of the average size of the aromatic units (La).

Keywords: A. Char, Semicoke; C. X-ray diffraction; D. Crystal structure, Electrical properties

1. Introduction

Aromatic hydrocarbons are major components of coal derived materials such as coal tar, coal pitch and carbonaceous solids when the materials are obtained below a temperature at which a high rate of hydrogen evolution can be noted. The temperature in question for various coal derived materials is within the 800–1200°C range [1]. Further heating may result in a content decrease of aromatic hydrocarbons on account of the formation of graphene layers. The aromatics present a variety of compounds with respect to molecular size and types such as peri- or kata-condensed aromatics, and oligomers. The latter refers to compounds that consist of aromatic units linked by a C–C bond. Intermolecular interactions between aromatics play an important role in processing and in the formation of the structure of the final products in carbonization processes.

Benzene–benzene interactions have been the subject of significant research effort at the theoretical level [2–9] since these interactions have been considered to be a prototype for interactions between other aromatic systems in chemistry, biology and physics. Studies referring to the interactions of other aromatic hydrocarbons are limited to toluene dimers [9]; benzene–naphthalene and benzene–anthracene dimers [4]; $(benzene)_n$–perylene and $(benzene)_n$–tetracene complexes for $n=1$ to 7 benzene molecules [10], and coronene dimers and circumcoronene dimers [11]. In the latter, [11], a method of calculating intermolecular forces was used that is exclusively applicable to aromatic molecules of D_{6h} symmetry; such highly symmetric aromatics can hardly be expected to be significant components of carbonaceous materials. Moreover, geometries of kekulene and annulene stacks were studied [12].

Consideration referring to the nature of the forces that

*Fax: +48-32-231-2831.

E-mail address: inbox@karboch.gliwice.pl (A. Marzec).

0008-6223/00/$ – see front matter
PII: S0008-6223(00)00024-5

are involved in interactions among aromatic hydrocarbons, included van der Waals dispersive interactions [3–9]; correlation interactions [5,7]; $\pi-\sigma$ attractive forces [12] (i.e., interactions between π electrons of a molecule and positively charged carbon nucleus in aromatic ring of another molecule), and quadrupole–quadrupole electrostatic forces [9].

It is worth pointing out that results referring to dimer configurations of low molecular weight hydrocarbons should NOT be extrapolated on aggregates of high molecular weight hydrocarbons. This was clearly shown by Chipot et al. [9] — benzene is not a good model even for toluene. Their calculated and experimental data indicated the preference for a T-shaped benzene dimer, but for toluene there was a definite preference for the stacked dimer. The reason for the different behavior of these two substances is as follows [9]. Quadrupole–quadrupole interactions are the predominant interactions in the benzene dimer; these interactions result in repulsion of the stacked dimers. In toluene, the attractive dispersion term, reinforced by the presence of the methyl group, counterbalances the unfavorable electrostatic quadrupole–quadrupole repulsion and, therefore, the stacked dimers are preferred over T-shaped. It is not possible to predict whether quadrupole–quadrupole forces or dispersive forces prevail in any high molecular weight aromatic hydrocarbon.

At present, software packages such as HyperChem have opened a possible way for direct studies on interactions in higher aromatic systems. The interactions can be studied with the use of a force field and geometry optimization. Using this procedure a molecule is described as a collection of atoms that interact with each other through a potential energy function. The potential energy of a molecule depends on bond lengths and angles, torsion angles as well as on interactions among nonbonded atoms that include van der Waals and coulombic forces. A minimum of the potential energy indicates stable conformers or stable aggregates of molecules.

In the present paper, the orbitals and the partial atomic charges of polynuclear benzenoid hydrocarbons (PAHs) as well as of aromatic oligomers were calculated with the use of selected semi-empirical methods of quantum chemistry. Numerous applications of quantum chemistry in the studies of PAHs with respect of their reactivity, were extensively reviewed by Zander [13,14]. Marzec [15] applied some semi-empirical methods for orbital calculations of low molecular oligomeric molecules.

2. Computational methodology

In the present paper, HyperChem software (Release 4.5 for Windows 3.11; Processor P 133 MHz; RAM 4×32 MB; HDD 850 MB) was applied in all molecular and quantum mechanics calculations. Major commands of the software, written in italics, are shown in brackets.

2.1. Aromatic molecules studied

The compounds that were the subject of the calculations belong to two groups of aromatics, namely to (i) high condensed aromatic hydrocarbons (PAH), and (ii) oligomeric molecules which consist of several aromatic units linked by C–C bonds.

The PAHs studied were arbitrarily selected out of a vast number of compounds identified in coal tar and pitch [16–18]. An example of the PAHs studied is shown in Fig. 1.

Information on the structure of the oligomers in coal derived products is limited to rather low molecular compounds such as biphenyl and phenylnaphthalene identified in coal tars [16]. A set of various analytical methods applied to coal tar pitch led to the conclusion that the number average molecular weight of pitch oligomers is approximately 1000 [18]. It may be assumed that oligomers in solid carbonaceous materials (such as active carbons and semicokes) have molecular sizes comparable with the latter. Due to the limited information available, oligomers studied in this work were just constructed using the assumption that they consist of aromatic units which represent typical tar components. Molecular masses of the oligomers studied were in the range of 600 to 1000 amu. Higher masses could not be handled by the computer in a reasonable time. An example of the oligomers is displayed in Fig. 2; the oligomer consists of two dibenzopyrenes, benzoacephenanthrylene and benzocarbazole (see for example, Ref. [17] for major tar components).

Two types of oligomers were constructed. Type 1-oligomer (see Fig. 2) was built in such a way that the molecule cannot undergo intramolecular cyclodehydrogenation reaction by forming 6- or 5-membered aromatic rings. On the contrary, the type 2-oligomer (see another isomer in the Figure) can form such aromatic rings and give rise in this way to a PAH molecule on heating. Studies on various biaryls that can be ascribed to type 2 showed they really undergo intramolecular cyclodehydrogenation [13,19,20]. According to Senthilnathan and Stein [19], the

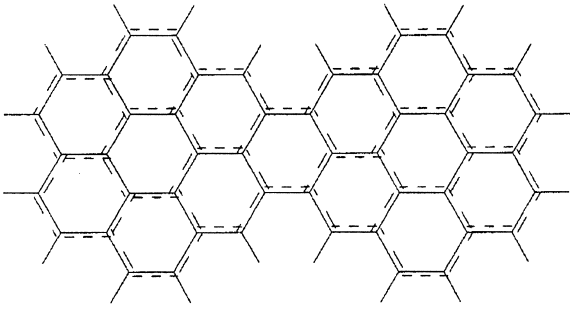

Fig. 1. An example of PAHs studied: Dicoronene (the largest aromatic compound that, as yet, has been detected in coal-tar pitch [18]). Molecular mass = 596 amu.

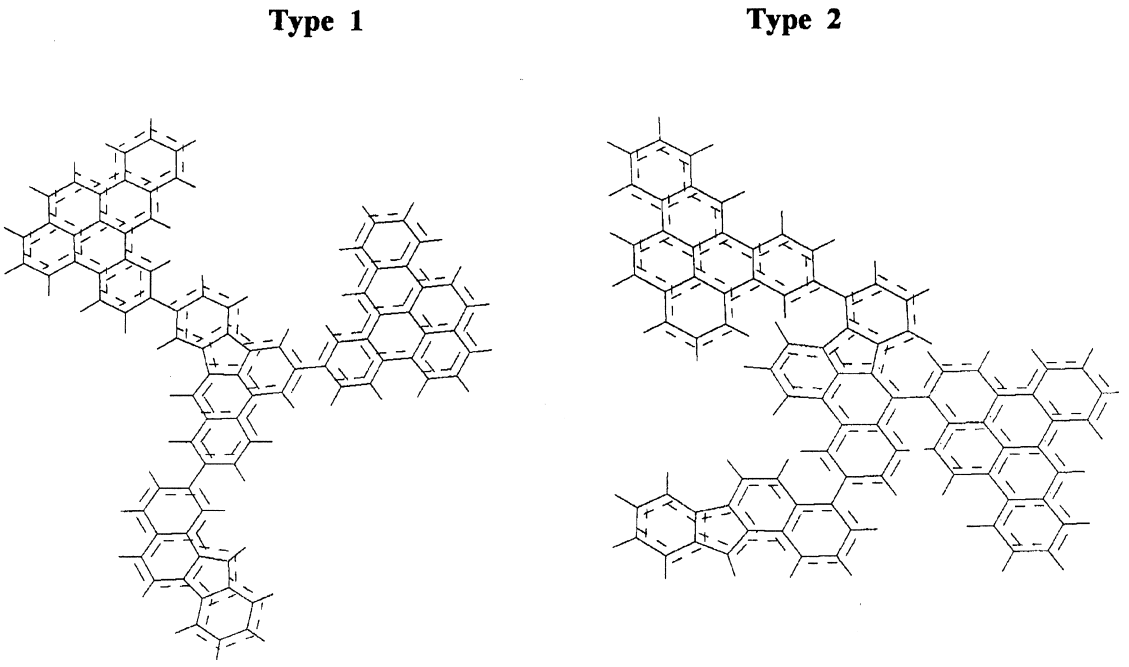

Fig. 2. An example of the oligomers studied. The oligomer displayed: (84 C + 1 N + 45 H); molecular mass = 1067 amu. Type 1: An isomer of the oligomer that cannot react via intramolecular dehydrocyclization (one of the energy minimized conformers of this isomer is displayed in Fig. 4). Type 2: Another isomer which can be a subject of the intramolecular dehydrocycliztion (one of its energy minimized conformers is also shown in Fig. 4).

intramolecular cyclodehydrogenation of biaryls is mediated by H-donors. Thus, it may be expected that such oligomers are preserved at least in coal derived materials which are deficient in H-donors. It is amazing, however, that such biaryls (bipyrenes were studied) and their products of intramolecular cyclodehydrogenation still coexisted at temperature as high as 1200 K [20].

There are no direct analytical data indicating that high molecular weight oligomers of both types are formed and exist in coal derived materials. However, studies carried out with the use of frontier orbitals theory on reactive sites in aromatic hydrocarbons (Marzec A.: Reactivities of hydrocarbons in terms of frontier orbitals theory; in preparation for publication) imply that the two types of oligomers, as well as oligomers consisting of both types, may be formed. Statistical factors make a preference for formation of the type 2-oligomers in higher content compared with the content of type 1. But the latter may be better preserved since they cannot undergo intramolecular cyclodehydrogenation.

2.2. Potential energy and geometry optimization for PAHs, oligomers and aggregates of the molecules

Calculations of the energy and geometry optimization was carried out with the use of MM+All Atom Force Field (MM+AAFF) and Steepest Descent algorithm (SD). The MM+AAFF is an extension of MM2 developed by Allinger [21] and his group. Using HyperChem [22] the calculations were carried out for all nonbonded interactions (*cutoffs none*), in ''gas phase'' mode. In fact interactions among two up to six molecules had been calculated. Solid carbonaceous products in general are porous materials that contain various pores (from ultramicropores <0.5 nm, micropores <2 nm to mesopores 2–50 nm and macropores >50 nm). The materials show high inner surface area in the range from a few hundred to ~2 000 m^2/g. Thus, potential energy calculations carried out in ''gas phase'' mode seem to be a more appropriate description of such porous systems, compared with to modes of liquid phase or solid phase with periodicity.

Geometry optimization finds the coordinates that represent a potential function minimum of a molecule or of aggregates of molecules. It also provides a gradient value (kcal mol^{-1} 0.1 nm^{-1}) which is the derivative of the energy with respect to all Cartesian coordinates. When the gradient is >0 the system is not in its energy minimum state. In the paper, only gradients of >0.1 are quoted.

Major HyperChem commands used: (*MM+; Charge; Geometry Optimization; Steepest Descent algorithm*).

2.3. Molecular orbitals and partial atomic charges

The charges were calculated for PAHs and the oligomers

using two semi-empirical methods (*ZINDO1; Single Point and MINDO3; Single Point* calculated MO; MINDO3 has proved very effective in studies of methane and ethane cations and reactions of hydrogen elimination [23]). The calculated partial atomic charges were then used in the MM+AAFF geometry optimization — SD procedure.

2.4. Conformational analysis of oligomers

In search for stable conformers of the oligomers the procedure applied was to perform the semi-empirical calculations of partial atomic charges (ZINDO1 and MINDO3) followed by the MM+AAFF geometry optimization — SD, followed by Molecular Dynamics (*Molecular Dynamics*). The latter was used with the exclusive aim to change torsion angles between aromatic units of an oligomer. Then, the cycles MM+AAFF — geometry optimization —SD, followed by Molecular Dynamics were repeated in order to find minima of potential energy of the oligomer conformers (*MM+; Charge: Geom. Opt.; Steepest D.*; potential energy and torsion angles read-outs; *Molecular Dynamics; MM+*, etc.).

2.5. Intermolecular interactions studied

The following interactions were studied: (i) Among PAH molecules; (ii) among oligomeric molecules, and (iii) among PAH and oligomer molecules. The energy of interaction in an aggregate E_i was calculated as a difference: $E_i = E - (E_1 + E_2 + \ldots . E_n)$ where: E is a minimum potential energy of the aggregate; $E_1 \ldots E_n$ are potential energies of individual molecules showing exactly the same conformation as they have in the energy optimized aggregate. The following information results from the E_i values: (i) Negative value of E_i indicates an aggregate of molecules that are united by attractive forces; (ii) the higher the absolute E_i value, the stronger the attractive forces.

It should be pointed out that the E_i values derived from the gas phase calculations cannot be directly compared to experimental enthalpies of sublimation or vaporization. To compare the calculated result with the experimental one, the effect of the zero-point energy should be also considered [5]. Other possibilities are as follows [8]: For calculating heat of sublimation one would need not only the E_i value but also a computed energy of a molecule in the crystallic state; for calculating heat of vaporization, the potential energy of a molecule in the liquid state should be computed.

3. Results and discussion

3.1. Benzene dimer interactions and configurations

With the aim of validating the present method, our results of calculations on the benzene dimers are compared with corresponding published data.

The benzene–benzene dimer interaction energies, calculated with the use of the present method and other ones [4,6–9] that include ab initio calculations, are compared (Table 1). The comparison shows the present energies for T-shaped dimer (-1.78 and -1.74) are in the range of the energies calculated by Hobza et al. [7] (-1.66) and by Nagy et al. [8] when the MM3 force field was applied (-1.89). For the parallel dimer, the present energies (-1.74 and -1.81) correspond with the energy calculated by Jorgensen et al. [4] (-1.70) and are between those calculated by Chipot et al. [9] (-1.30 and -2.13). For the parallel-displaced dimer, the present results (-1.71 and -1.76) are between those calculated by Hobza [7] (-1.98) and calculated by Nagy [8] when the MM2b force field was applied (-1.65).

As shown in the review, [6], of experimental techniques yielding information on configurations of benzene–benzene dimers, the problem has not been definitely clarified. T-shaped and parallel-displaced dimers were experimentally detected however, a presence of another configuration could not be excluded. The same can be derived from comparison of experimental and calculated results, presented by Chipot (see page 11 221 in Ref. [9]).

The data in Table 1 shows that taking into account the calculated energies, the conclusions derived from various theoretical calculations are also not consistent. Some of them indicate the T-shaped configuration being the most stable, others prefer parallel-displaced. Our calculations (see Table 1) indicate either T-shaped or parallel (not displaced) configurations being the most stable, depending on the methods used (MINDO3 or ZINDO1) for partial atomic charges calculations.

Summing up, the calculation results for the benzene dimer obtained with the use of the present method are within the range specified by the other methods based on various force fields or ab initio calculations.

With respect to other hydrocarbons, the interaction energies for benzene–naphthalene and benzene–anthracene dimers were also calculated and compared with the published data [4]. According to the Jorgensen's results (see Fig. 14 in Ref. [4]), the T-shaped benzene–naphthalene dimer was slightly more stable than the stacked dimer ($\Delta E = -0.32$ kcal/mol). However, upon increasing the system size to anthracene the interaction energy values showed a stability preference for the stacked dimer of benzene–anthracene compared with the T-shaped one. Our calculations showed the preference for the stacked configuration in both cases, i.e., in benzene–naphthalene as well as in benzene–anthracene dimers.

3.2. Partial atomic charges in PAHs and oligomers

The charges were calculated for numerous PAHs including dicoronene and the oligomers. The calculated charges

Table 1
Interaction energies (kcal/mol) for different configurations of the benzene dimer

	Configuration of benzene dimer		
Source	T-shaped	Parallel	Parallel-displaced
Ref. [4][a]	−2.15	−1.70	−2.11
		ab initio:	
Ref. [7][b]	−1.66	−0.85	−1.98
Ref. [8][c]	−2.21 (WS 77)	–	−2.11 (WS 77)
	−2.10 (MM3bmccr)	–	−2.55 (MM3bmccr)
	−1.89 (MM3)	–	−1.65 (MM2b)
Ref. [9]	−2.27	−1.30	
		ab initio:	
	−2.84	−2.13	
HyperChem-present method[d]	For partial atomic charges derived from ZINDO1:		
			−1.48 (displacement as in [4])
	−1.78	−1.74	−1.71 (displacement as in [7])
	For partial atomic charges derived from MINDO3:		
			−1.48 (displacement as in [4])
	−1.74	−1.81	−1.76 (displacement as in [7])

[a] See Fig. 1 in Ref. [4].
[b] See Table 2 in Ref. [7].
[c] See Table 2 in Ref. [8]; the paper presents critical evaluation of various force fields.
[d] See Section 2.

in the hydrocarbons were of the order of few electron charge units $\times 10^{-2}$ or $\times 10^{-3}$. The higher values were observed when they were derived from ZINDO1. The differences (between MINDO3 and ZINDO1 charges) had no significant effect on the results of geometry optimization.

3.3. Interactions among PAHs

Our calculations for selected T-shaped, parallel and parallel-displaced PAHs agglomerates showed that the T-shaped ones were definitely less stable. This is in accordance with the key message of Jorgensen [4] that ''stacked structures become more favorable with increasing size of arenes''. Therefore, further work had been concentrated on PAHs parallel and parallel-displaced stacks which, no doubt, show links with the optical anisotropic phase in hydrogen containing carbonaceous materials.

With regard to displacement, there was not any significant difference of potential energy between parallel stacks and the stacks showing small displacement. For example, the minimal energies for the stacks of four coronene molecules were as follows:

- E = −186.335 kcal for parallel, not displaced stack (i.e., face to face configuration);
- E = −186.226 kcal for parallel planes shifted 0.1 nm to each other;
- E = −181.183 kcal for parallel planes shifted 0.2 nm to each other; thus, the 0.2 nm shift yielded already a considerable change of energy.

Therefore, it is concluded that, in realistic systems of PAHs in carbonaceous materials, parallel and parallel-slightly displaced configurations show stability preference over extensively displaced stacks.

The energy minimized stacks of various PAHs showed interlayer distances in the 0.32–0.37 nm range between aromatic planes. The values (in this range) depended on the PAH structure (kata- or peri-condensed; symmetrical or not symmetrical) and, to some extent, on configuration of PAHs stacks (parallel or parallel-displaced). Molecular weight of the PAHs had no significant effect on the interlayer distances.

The results correspond well with experimental measurements of interlayer spacing of various carbonaceous materials. Thus, for graphite the spacing was 0.335 nm (see for example, Ref. [24]); for crystals of large aromatic hydrocarbons (10 to 15 condensed aromatic rings) the spacing was 0.336 to 0.346 [25]; for aromatic units (3–5 condensed aromatic rings) in vitrinites the spacings were in the 0.34 to 0.38 nm range [26]; and for carbonaceous materials prepared by carbonization of various individual

PAHs the spacing was 0.335–0.347 nm [27]. The consistency of the calculated (0.32–0.37 nm) and the experimental interlayer spacings (0.33–0.38 nm) indicates that the method applied in this work yields realistic systems of aromatic aggregates.

It is worth pointing out that when geometry optimization was carried out with the use of the semi-empirical methods (AM1 and PM3 were also included), instead of the MM+ AA Force Field, the methods resulted in larger intermolecular distances when compared with the experimental distances.

An example of the energy E_i of molecular interactions is presented: The potential energy E for the energy optimized stack of four dibenzopyrene molecules was −131 kcal: E_i was −56 kcal. The negative sign indicates the stack is united by intermolecular attractive forces. The forces should be ascribed to van der Waals dispersive interactions since only a very low contribution of coulombic forces could be expected due to the low partial atomic charges in aromatic hydrocarbons (see Section 3.2).

3.4. Molecular orbitals of PAH stacks

Fig. 3 shows, as an example, two orbitals (out of the total number of 330 molecular orbitals) of the energy minimized stack of three dibenzopyrene molecules ($E = -95$ kcal; $E_i = -37$ kcal). The three molecules in the stack are united by the π-orbitals shown. In fact, the stack has more common orbitals (i.e., the orbitals shared by individual molecules).

Results obtained for the energy optimized aggregates of other PAHs were the same with respect to the occurrence of common molecular orbitals. It should be emphasized that, no matter which semi-empirical method was used (MINDO3, ZINDO1, as well as occasionally AM1 and PM3), there was always a number of common orbitals within a PAH stack. When interlayer distances were made (manually) larger, the number of common orbitals decreased and, finally, at distances >0.5 nm only separate orbitals for the separate molecules were seen.

The lowest HOMO–LUMO energy gaps were observed at the interlayer distance of 0.32 nm and the gaps were sharply increasing as the distance increased. Values of the energy gaps are not quoted since the different semi-empirical methods yielded quite different energy gaps.

Thus, the four semi-empirical methods are in accordance in a qualitative sense: All of them reveal an occurrence of common orbitals. In a quanitative sense, they are not in accordance: the orbital energies and HOMO–LUMO gaps are quite different.

The occurrence of common orbitals indicates that some electrons in the aromatic stacks can be delocalized within an array of carbon atoms although the atoms belong in fact, to individual molecules.

3.5. Conformation of type 1-oligomer

Calculations showed that potential energy value E of the planar oligomer (displayed in Fig. 2) was +16 kcal/mol and the gradient was 14.8 kcal/mol/0.1 nm. This indicates that the planar conformer is not in its energy minimum state. The conformer is influenced by repulsive forces acting within the molecule. Further calculations (the cycles *Molecular Dynamics — MM+AAFF — Geometry Opt.*) revealed a flat and wide plateau of potential energy (from −34 to −39 kcal/mol) when torsion angles in the molecule were in the 4° to 40° range (Fig. 4 displays one such conformer). Thus, the molecule is flexible and its part can be almost flattened since torsion angles in the range in question may be changed by supplying a few kcal. An

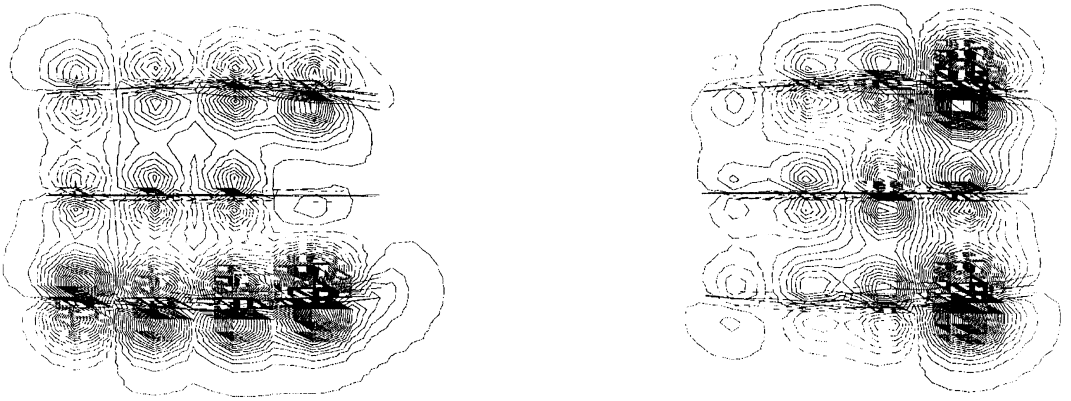

Fig. 3. Potential energy minimized stack of three dibenzopyrene molecules. Two examples of orbitals shared by the three molecules are displayed.

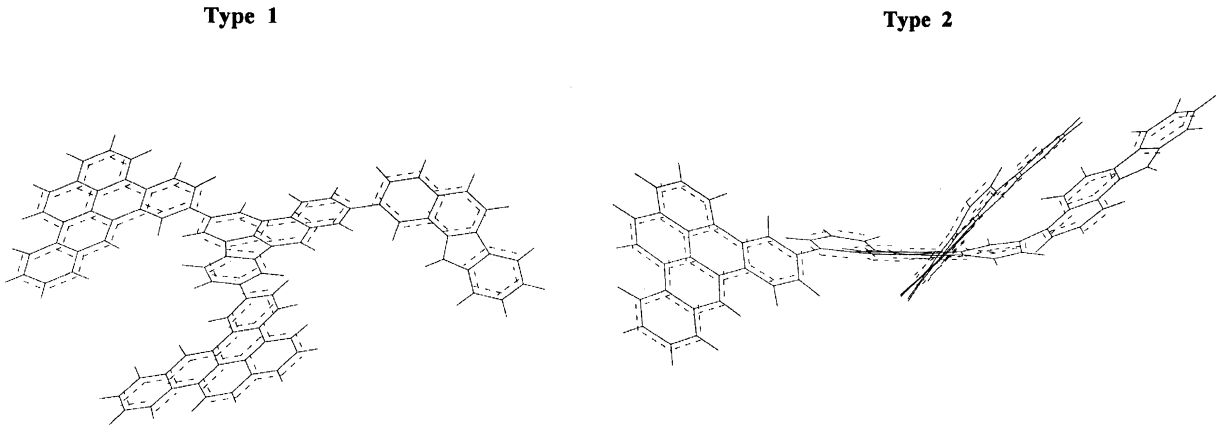

Fig. 4. Examples of energy minimized conformers of oligomers. Type 1-oligomer: Torsion angles are 23, 20 and 17°; $E=-39$ kcal (compare with $E=+16$ kcal for the planar conformer). Type 2-oligomer: Torsion angles are 36, 37 and 52; $E=-13$ kcal (compare with $E=+3730$ kcal for its planar conformer).

increase of the potential energy was observed when the torsion angles were beyond the 4°–40° range.

3.6. Conformation of type 2-oligomer

Potential energy value of the oligomer in its planar conformation (see the conformation in Fig. 2) is very high: $E=+3730$; gradient $=257$ kcal/mol/0.1 nm. This indicates strong repulsive forces which are mostly due to short distances (about 0.05 nm) between some hydrogen atoms on the adjacent aromatic units. Hence, the planar conformer is not a stable one. After the application of the same procedure as for type 1-oligomer, local energy minima, from -3 to -15 kcal/mol were found when torsion angles were in the 30°–65° range (one of the conformers is displayed in Fig. 4). Below 30°, the molecule had positive values of potential energy. This indicates that eventual flattening of the type 2-oligomers would need much higher energy input compared with the oligomers of type 1.

3.7. Molecular orbitals of the oligomers

The orbitals of the oligomers had been calculated for their non-planar, energy minimized conformers. π-orbitals were found between C atoms that form a C–C link between two aromatic units (although the units were not co-planar). This indicates that the C–C bonds have a double bond character to some extent (the order of the bonds in question were not calculated). The results also indicate that extended delocalized π-orbitals (over individual aromatic units) occur in high molecular weight oligomers when torsion angles between the units are not too high ($<60°$). Information on this issue that refers to di-, tri- and tetramers of low molecular aromatic hydrocarbons was already published [15].

3.8. Intermolecular forces among oligomers

Fig. 5 (left) shows the aggregate of five oligomeric molecules (type 2) in the state characteristic for one of the local energy minima. The potential energy of the aggregate is $E=-82$ kcal. The difference $E_i=-39$ kcal indicates the attractive interactions among the molecules in the aggregate. As the figure displays, the oligomeric macromolecules in the aggregate preserve their non-planarity. It is also worth pointing out that the molecules can hardly be arranged with respect to each other in such way that they would form stacks of parallel aromatic layers. This implies that such oligomeric aggregates form an optically isotropic phase in carbonaceous materials.

Due to some change of their conformation by intermolecular forces, aggregates of type 1-oligomers (not displayed) showed a few parallel aromatic units; the interlayer distances between the units were in the 0.35 to 0.58 nm range. Thus, these aggregates may show small domains of optical anisotropy while a larger part of the aggregate is isotropic.

3.9. Intermolecular forces among PAHs and oligomers

The same procedure was applied for studying aggregates of the type 2-oligomer and dicoronene. Fig. 5 (right) shows one of the energy minimized aggregate of the type 2-oligomer and three dicoronene molecules. The potential energy of the aggregate $E=-266$ kcal. The energy difference is $E_i=-54$ kcal. The dicoronenes became almost parallel relative to the aromatic units of the

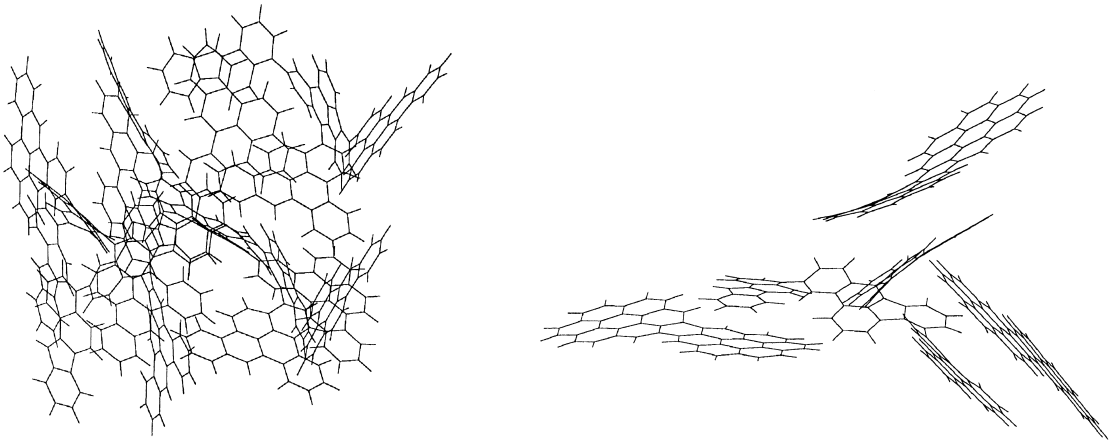

Fig. 5. Energy minimized aggregates of: (Left) Five oligomeric molecules ($E=-82$ kcal; $E_i=-39$ kcal); (Right) an oligomer and three dicoronenes ($E=-266$ kcal; $E_i=-54$ kcal).

oligomer. The distances between the ''parallel'' planes were 0.35 to 0.4 nm.

The first point to emphasize is that the molecules of dicoronene and the aromatic units of the oligomer are deviated from planarity (see, for example, the upper dicoronene in Fig. 5). Such deviations were always noted when one part of a large aromatic plane was influenced by a stronger intermolecular force than another part. Only a few kcal are needed for such deviation. For example, the potential energies of the three non-planar dicoronenes in Fig. 5 are from -66.9 to -68.9 kcal/mol compared with the energy of the planar one which is -69.2 kcal.

The second point is that an oligomeric molecule can play the role of a nucleus around which aromatic hydrocarbons (PAHs) are arranged in various spatial directions, reflecting the space orientation of the oligomer aromatic units.

4. Summary and conclusions

Application of the method described in Section 2 to aggregates of PAH molecules resulted in the formation of parallel stacks (crystallites) with interlayer spacings in the 0.32 to 0.37 nm range. The interlayer distances correspond with the experimentally measured distances for various carbonaceous materials [24–27]. This consistency as well as the comparison of the results for benzene dimers obtained with the use of the present and other force fields [4,7–9] indicates that the application of the method to aggregates of aromatic molecules is justified.

The method in question applied to aromatic oligomers showed that the oligomers are not planar molecules no matter what was their molecular size. In aggregates of oligomers, parallel stacks of aromatic units scarcely occur.

In mixed PAH/oligomer aggregates, the PAH molecules are arranged parallel to aromatic units of the oligomer, reflecting various spatial orientations of the oligomer units.

These results contribute to the explanation of the poorly known chemical nature of the optically isotropic phase in carbonaceous materials (in contrast to the chemical nature of the anisotropic phase which is well known to be made of stacks of parallel PAHs). Thus, from the molecular mechanics point of view, the isotropic phase is composed of oligomeric aggregates and/or of mixed PAH/oligomer aggregates.

The arrangements of PAHs around oligomeric molecules displayed by molecular mechanics (see Section 3.9) corresponds with (a) the schematic representation (derived from X-ray measurements) of non-graphitizing carbons [28], and (b) with Oberlin's model of some TEM microtexture domains in cokes that is called the ''crumpled sheets of paper'' model [29]. Thus, these materials are likely composed of mixed aggregates of PAHs and oligomers that are highly dispersed in the former.

Large aromatic planes can be easily deviated from planarity when one part of the plane is influenced by stronger intermolecular force than another part (see Section 3.9). The deviation of aromatic units from planarity may result in erroneous estimation by X-ray measurements of average size of aromatic units (L_a) in carbonaceous materials. The size may be, in fact, larger compared with the size derived from X-ray measurements.

The application of semi-empirical quantum chemistry methods revealed common orbitals in the stacks of parallel aromatic units, whether or not the stacks are formed by PAH molecules or they occur in aggregates of oligomers, or in mixtures of PAHs and oligomers. The orbitals in question make orbital links among individual molecules which unite the molecules by means of delocalized electrons. The occurence of the common orbitals may be one of a number of phenomena that contribute to some

electrical conductivity of non-graphitic carbonaceous materials [30].

Acknowledgements

The author is greatly indebted to Professor Doctor St. Kucharski of Silesian University in Katowice for reading the manuscript and his valuable comments. Financial support by KBN Grant no. 3 TO9A 003 13 is acknowledged.

References

[1] Stanczyk K, Boudou JP. Fuel 1994;73:940–4.
[2] Williams DE, Starr TL. Comput Chem 1977;1:173–7.
[3] Jorgensen WL, Madura JD, Swenson CJ. J Am Chem Soc 1984;106:6638–46.
[4] Jorgensen WL, Severance DL. J Am Chem Soc 1990;112:4768–74.
[5] Hobza P, Selzle HL, Schlag EW. J Phys Chem 1993;97:3937–8.
[6] Hobza P, Selzle HL, Schlag EW. Chem Rev 1994;94:1767–85.
[7] Hobza P, Selzle HL, Schlag EW. J Am Chem 1994;116:3500–6.
[8] Nagy J, Smith VH, Weaver DF. J Phys Chem 1995;99:13868–75.
[9] Chipot Ch, Jaffe R, Maigret B, Pearlman DA, Kollman PA. J Am Chem Soc 1996;118:11217–23.
[10] Lohmannsroben HG, Bahatt D, Even U. J Phys Chem 1990;94:6286–90.
[11] Miller JH, Mallard WG, Smyth KC. J Phys Chem 1984;88:4963–70.
[12] Hunter CA, Sanders JKM. J Am Chem Soc 1990;112:5525–34.
[13] Zander M. Physical and chemical properties of polycyclic aromatic hydrocarbons. In: Bjorseth A, editor, Handbook of polycyclic aromatic hydrocarbons, New York: Dekker, 1983, pp. 1–25, and references therein.
[14] Zander M. Top Curr Chem 1990;153:101–22.
[15] Marzec A. Energy Fuels 1997;11:837–42.
[16] Anderson HC, Wu WRK. Properties of compounds in coal-carbonization products, Washington DC: Bureau of Mines, 1963, Bulletin 606.
[17] Blumer SP, Thoms R, Zander M. Erdoel und Kohle 1978;31:197.
[18] Zander M. Pitch characterization for industrial applications. In: Marsh H, Heintz EA, Rodriguez-Reinoso F, editors, Introduction to carbon technologies, Alicante: Universidad de Alicante, 1997, pp. 425–460; and references therein.
[19] Senthilnathan VP, Stein S. J Org Chem 1988;53:3000–7.
[20] Mulholand JA, Mukherjee J, Sarofim AF. Energy Fuels 1997;11:392–5.
[21] Allinger NL. Molecular mechanics, Washington DC: American Chemical Society, 1982, ACS monograph no. 177.
[22] HyperChem – computational chemistry – molecular visualization and simulation, Hypercube Inc, 1994.
[23] Dewar MJS, Rzepa HS. J Am Chem Soc 1977;99:7432.
[24] Ruland W. X-ray diffraction studies on carbon and graphite. In: Walker PL, editor, Chemistry and physics of carbon, Vol. 4, New York: Dekker, 1968, pp. 1–84.
[25] Goddard R, Haenel MW, Herndon WC, Krueger C, Zander M. J Am Chem Soc 1995;117:30–41.
[26] van Krevelen DW. In: Coal-Typology-Physics-Chemistry-Constitution, Amsterdam: Elsevier, 1993, p. 234.
[27] Fitzer E, Mueller K, Schaefer W. In: Walker PL, editor, Chemistry and physics of carbon, New York: Dekker, 1971, pp. 355–61.
[28] van Krevelen DW. In: Coal-Typology-Physics-Chemistry-Constitution, Amsterdam: Elsevier, 1993, pp. 238–9.
[29] Rouzaud JN. Fuel Process Technol 1990;24:55–69.
[30] Marzec A, Czajkowska S, Moszynski J. Energy Fuels 1994;8:1296–303.